© EARSeL and Warsaw University, Warsaw 2005. *Proceedings of 4th EARSeL Workshop on Imaging Spectroscopy. New quality in environmental studies.* Zagajewski B., Sobczak M., Wrzesień M., (eds)

SPECTRAL DETERMINATION OF PLANT WATER CONTENT OF WHEAT CANOPIES

Ruth Sonnenschein[1], Thomas Jarmer[2], Michael Vohland[3] and Willy Werner[4]

1. Remote Sensing Department, University of Trier, D-54286 Trier, Germany, ruthsonnenschein@gmx.de
2. Remote Sensing Department, University of Trier, D-54286 Trier, Germany; jarmer@uni-trier.de
3. Remote Sensing Department, University of Trier, D-54286 Trier, Germany; vohland@uni-trier.de
4. Department of Geobotany, University of Trier, D-54286 Trier, Germany; werner@uni-trier.de

ABSTRACT

The aim of this study is to analyse the relationship between spectral reflectance measurements and the water content of wheat canopies based on the Water Index WI (R900/R970) of Peñuelas et al. (i) and a modified version of this index. For this purpose, reflectance measurements over a full phenological cycle of four wheat canopies using an ASD FieldSpec II spectroradiometer have been performed. Canopy water content has been determined by the difference between fresh and dry weight of the harvested plant material.

Reflectance spectra were used to calculate both the WI and the modified WI-version. Both indices were compared for their prediction power of canopy water content using an exponential regression model. Final estimation results with cross-validated r^2 higher than 0.85 imply a possible operational application.

Additionally, the reflectance spectra were resampled to the HyMAP channels and the WI was then calculated from these spectra. The resulting exponential regression model was applied to HyMAP image data for spatial prediction of wheat canopy water content.

Keywords: Canopy water content, spectrometry, HyMAP, wheat

INTRODUCTION

For a balanced water supply is essential for plant development, the determination of plant water status is an important issue. Several experimental attempts have been made in the past (ii), but most of them suffer from time intensity and a lack of operationality. Thus, the development of adapted approaches for a rapid analysis is necessary.

In principle, there are two conceptually different approaches for the assessment of plant water status by means of remote sensing. One of them uses the thermal radiation emitted by canopies for detecting water stress (iii), whereas the other exploits the reflective spectral range. This study focusses on the latter approach which is based on the absorption process of the electromagnetic radiation by the plant water and uses its characteristic absorption features in the near and middle infrared.

The water content may either be determined by inversion of radiative transfer models (iv,v) or by empirical approaches (vi,vii). As the modelling approach is generally based on the knowledge of the interaction between radiation and leaf and allows a physical insight into the system behaviour it is often preferred.

On the other hand, the empirical methods generate a statistical relationship between spectral measurement and water content. These methods are quite simple and easy to use, but suffer from limitations under variable measurement conditions; therefore, they have to be recalibrated before being transferred to other regions or times (viii).

In general, spectral indices (vi,vii), parameters of the absorption features (ix,x) and spectral matching techniques (xi) can be distinguished. Among these empirical-statistical approaches, the spectral index might be most relevant for operational use for its simplicity and fast computation. Thus, the WI introduced by Peñuelas et al. (i) was chosen for analysis.

MATERIAL AND METHODS

Study area and field data

In the year 2000, four commercial winter wheat fields in the Bitburger Gutland were investigated for the complete phenological cycle; the Bitburger Gutland is located about 20 km north of Trier (Rhineland-Palatinate) in the south-west of Germany (figure 1). In each field three sub-plots with an area of 40 x 40 cm² were randomly selected. Measurements were taken during the vegetative (DOY 115, 130), the generative (160, 172) and the reproductive growth stage (DOY 213).

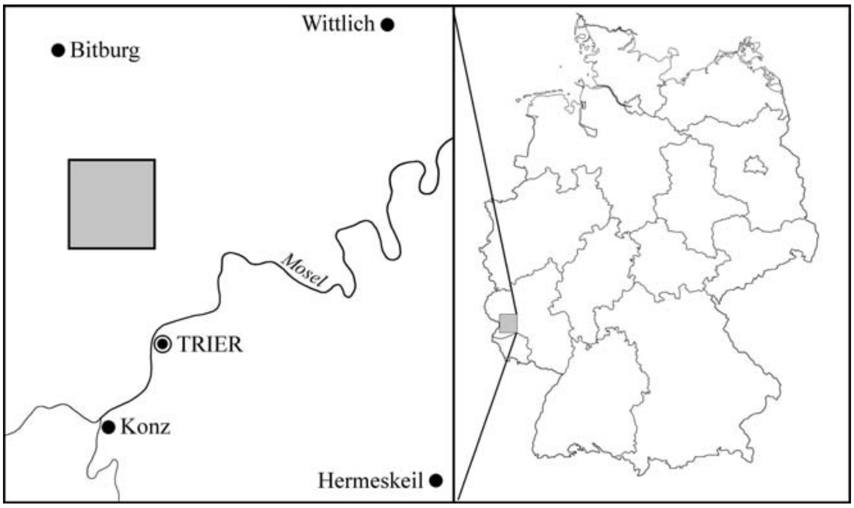

Figure 1: The location of the Bitburger Gutland

Radiometric spectra were obtained close to noon using a portable ASD FieldSpec II radiometer (Analytical Spectral Devices). The instrument allows reflectance measurements in the range from 350 to 2500 nm with a spectral resolution of 3 to 10 nm and a sampling interval of 1 nm. The radiometer was positioned at nadir (0°) about 1.5 m directly above the wheat canopy surface, the field of view was 25°. The spectral measurements were converted into absolute reflectance values using a spectralon reference panel of known reflectivity. Three measurements were taken for each sub-plot and the average was calculated. Due to sensor noise, spectra below 420 nm and above 2400 nm as well as the water vapour absorption features (1340-1450 nm, 1750-1970 nm) were eliminated. To minimize sensor noise, a moving Savitzky-Golay algorithm was applied to the remaining reflectance spectra using a third order polynom and a filter range of 31 nm (xii).

After collecting the spectra, the wheat plots were harvested and the plant material was packed carefully to avoid water loss. In the laboratory, the plant material was weighed first (fresh weight, FW) and, after being dried at 105°C for 24 hours, the dry weight for each plot (DW) was determined. Canopy water content (CWC) was then calculated by substracting DW from FW:

$$CWC = FW - DW [g/m^2] \quad (1)$$

Data processing

The water absorption features in the near and middle infrared are overtones and combinations of the three fundamentals of the water molecule and therefore differ in their strength. The quite strong absorption features in the middle infrared (1400 nm, 1900 nm, 2500 nm) may not be used under field conditions as the electromagnetic radiation is strongly influenced by the highly variable water vapour content in the atmosphere. On the other hand, the remaining absorption features at 970 nm and 1200 nm are only weakly developed but less influenced by atmospheric water vapour and hence, suitable for evaluation. Their strength and position in the electromagnetic spectrum result in another advantage. As the reflectance pattern of leaves in the near infrared is dominated by the characteristic volume scattering, the incoming solar radiation penetrates the canopy to a high degree, which leads to late saturation and high dynamics of the detectable reflectance signal (xiii).

In the run-up to this study there were no differences in the evaluation of both water absorption features (xiv). Therefore, focus was laid on the absorption feature at about 970 nm. The spectral index introduced by Peñuelas et al. (v) requires reflectance values at two different wavelengths: 970 nm (typical wavelength for the absorption feature) and another one at the plateau of the near infrared (900nm).

$$WI = \frac{R900}{R970} \tag{2}$$

The studies of Penuelas et al. (v,i) imply that the wavelength of maximum absorption varies by water stress. The same statement is also valid during the vegetation period (xv). So, a modification of the water index is calculated which uses the exact reflectance value of maximum absorption instead of the static wavelength at 970nm.

$$WI_{\mathrm{var}} = \frac{R900}{R_{\min(930-990)}} \tag{3}$$

The validation of the statistical relationships was done by cross-validation (leave-one-out method). The criteria r² and RMSE were chosen to assess the quality of the prediction models.

RESULTS

Figure 2 shows the empirical relation between the water indices and the canopy water content. The range is 0.98 to 1.26 for the WI and 0.98 to 1.27 for the modified WI version. With small water contents the values of both indices are not differing significantly. Obviously, there is a close relationship between both indices and the water content which is characterised by a strong slope for smaller water contents. For higher water contents, the tendency of saturation is evident for both indices.

The three measurements of the DOY 213 (marked) show significant differences of the common relationship. Although the measured canopy water contents range between 1380 g/m² and 2100 g/m², the indices show the absolute lowest values. For there are only three measurements of the canopy water content available for this date, it is questionable whether they can be assumed representative for the actual growth stage. The winter wheat is almost senescent which can be seen in the corresponding reflectance spectra characterised by low chlorophyll absorption indicating low photosynthetic activity. This coincides with the phenological observations of the German Meteorological Service (DWD) which state DOY 213 as the beginning of the harvest (xvi). Another reason for the outstanding values might be the geometry of the spectral measurements: In the growth stage of senescence nearly all water is contained in the grain, ears and stalks. As these plant elements are vertical orientated, their proportion in the sensor's field of view is small. Thus, the water content has to be underestimated by any spectral evaluation. For the yield, the water supply at senescence is not as important as during vegetative and generative growth stages; as consequence, the analysis concentrated on the water content of vital vegetation and the samples of DOY 213 were eliminated.

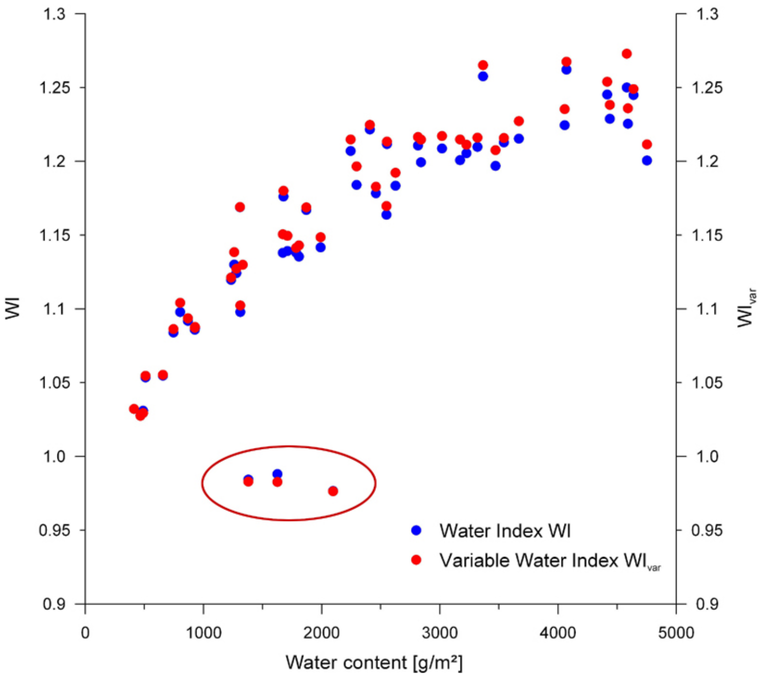

Figure 2: Relationship between water index, modified water index and canopy water content.

The relationship between water content and indices shows a trend of saturating indices for high water contents. Therefore, exponential models were used for prediction:

$$CWC = 0.013 * e^{10.24*WI} \quad (4)$$

$$CWC = 0.0196 * e^{9.83*WI_{var}} \quad (5)$$

For both indices, there is only a small scatter with small water contents. The highest deviations of the 1:1 line occur for high canopy water amounts. There are three samples – two of them obtained at DOY 160 and one at DOY 172 – with obviously outstanding errors of estimated water contents. All canopy parameters like LAI, PAI, fresh and dry weight were examined for these dates, but no reason was found for explanation. As the spectral measurements were performed under field conditions, there might be sampling mistakes not explainable retrospectively. The three samples were regarded as ‘outliers’ and eliminated.

The following equations are based on the remaining 45 samples:

$$CWC = 0.0095 * e^{10.507*WI} \quad (6)$$

$$CWC = 0.0156 * e^{10.033*WI_{var}} \quad (7)$$

According to these equations, r^2_{cv} was 0.896 and the $RMSE_{cv}$ was 405 g/m² for the WI. The prediction accuracy of the variable water index is nearly the same with r^2_{cv} = 0.869 and $RMSE_{cv}$ = 457 g/m².

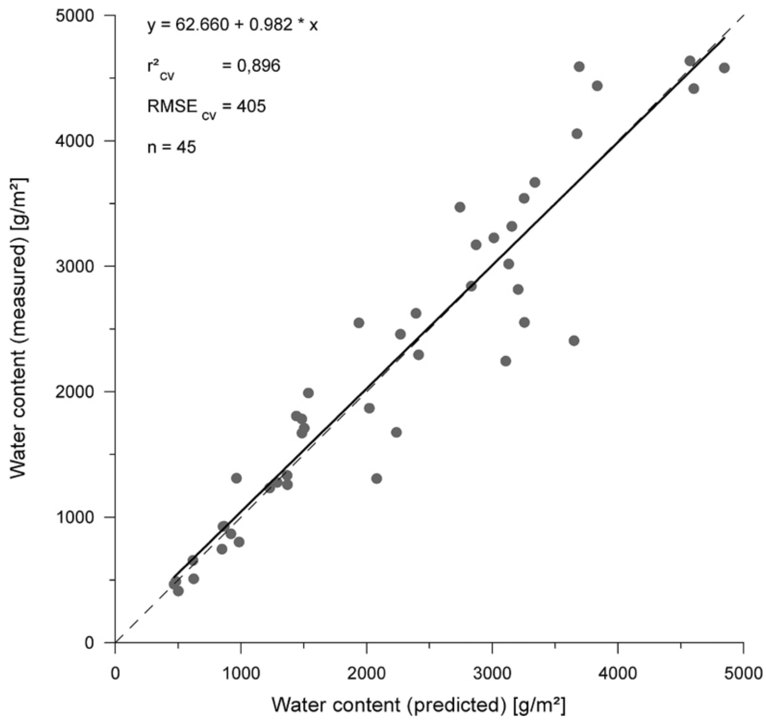

Figure 3: Scatterplot with estimated versus measured water contents of wheat canopies based on the Water Index WI (after cross-validation)

IMAGING SPECTROMETRY

The previous results were based on spectroradiometric "in situ"-measurements with a limited number of samples. The second aim of this study was to test whether these results could be transferred to imaging spectrometer data.

Unfortunately, no hyperspectral image data could be acquired during the field campaign in 2000. Nevertheless, data of the airborne HyMAP™ sensor from 1999 (June 10^{th}) with a ground resolution of 5 m could be integrated in this study. By HyMAP, the spectral range from 400 to 2,500nm is detected in 128 channels with a bandwidth from 13.7 to 24.3 nm (xvii). The pre-processing chain included the cross-track illumination correction and both atmospheric and geometric correction steps using ENVI's atmospheric correction module FLAASH and the PARGE™ software (xviii). The FLAASH module incorporates the MODTRAN 4 radiation transfer code (xix). For the flat terrain of the investigated plots, topographic normalisation was not performed (figure 6, left).

Analysis of synthetic HyMAP data

In a first step, continuous reflectance spectra were resampled to the central wavebands of the HyMAP sensor to simulate "synthetic" HyMAP data. For calculating the WI the HyMAP sensor offers reflectance measurements at 900 nm (channel 34), but there's no channel with 970 nm as central wavelength. Therefore, the WI has to be calculated using the HyMAP channels at 965 nm (channel 38) or 981 nm (channel 39) instead. The latter is preferred, because its bandwidth of 16.5 nm offers a complete measurement in the region of water absorption, whereas the 965 nm-channel with a bandwith of 25 nm is strongly influenced by the edge of decreasing reflectances from the infrared plateau to the water absorption feature.

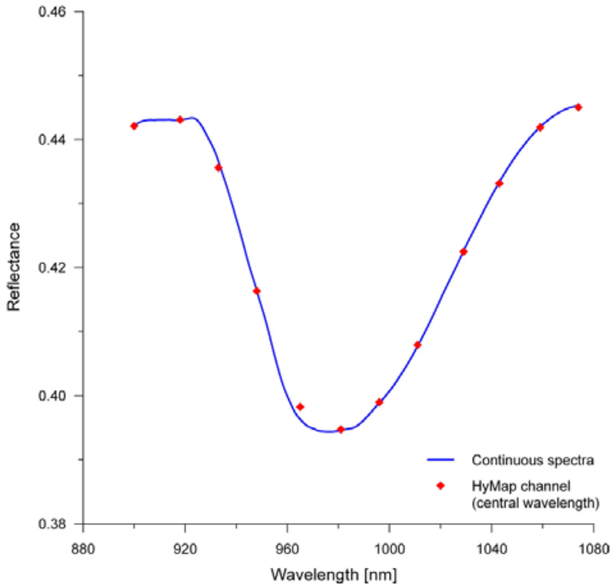

Figure 4: Comparison between reflectance from spectrometer measurements and simulated HyMAP bands (central wavelength position) in the region of water absorption at 970 nm

In the following the water index was calculated for channel 34 and 39 and a regression model was used to predict the canopy water content:

$$CWC = 0.0192 * e^{9.8703 * WI_{[900nm,981nm]}} \quad (8)$$

Based on this equation r^2_{cv} between predicted and measured values was 0.901 and $RMSE_{cv}$ was 398 g/m² (figure 5). Hence, the model quality for the simulated HyMAP data was very similar to the results achieved using the original WI.

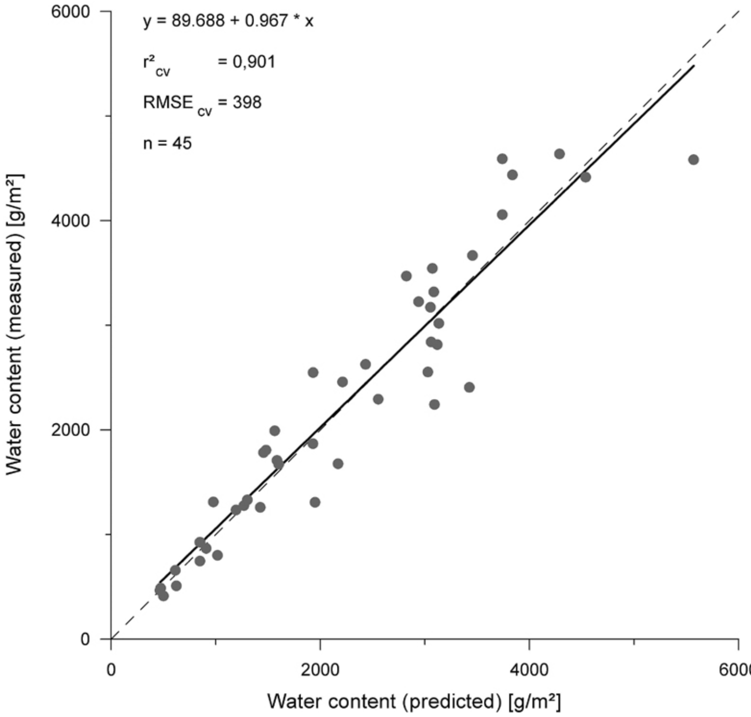

Figure 5: Scatterplot for cross validation of the model for water content of wheat canopies

Water content estimation based on HyMAP image data

To test the appoach described above, the water index using 900 and 981 nm was used for the image-based prediction of the canopy water content. First, the pixel-wise ratio between these reflectance values was calculated (figure 6, right). Unfortunately, most of the HyMAP image was clouded and in the cloud-free regions wheat was cultivated only on a very limited number of fields in 1999. For further analysis, one field was selected.

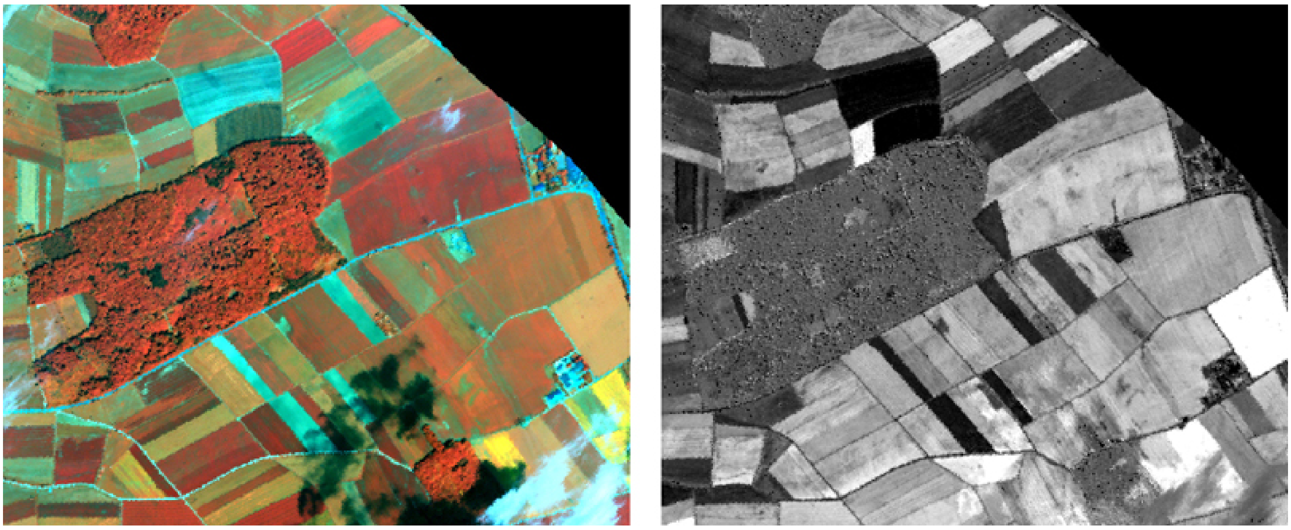

Figure 6: Subset of HyMAP image (left) and calculated water index (right)

Application of the established regression model to the HyMAP data is shown in figure 7. The estimated canopy water contents show a range quite similar to the values mesured in the year 2000. Highest canopy water contents (> 5000 g/m²) occur in some sinks in the centre of the field and on the eastern edge; they seem to be realistic, because water supply in these field segments is enlargened by lateral water flows. Lower contents (2000 - 3000 g/m²) were predicted for the northern and southern fringes of the field while the lowest values (< 2000 g/m²) were estimated for some small spots with low productivity. However, for the lack of reference measurements at the time of overflight, no direct validation of the predicted water contents was possible.

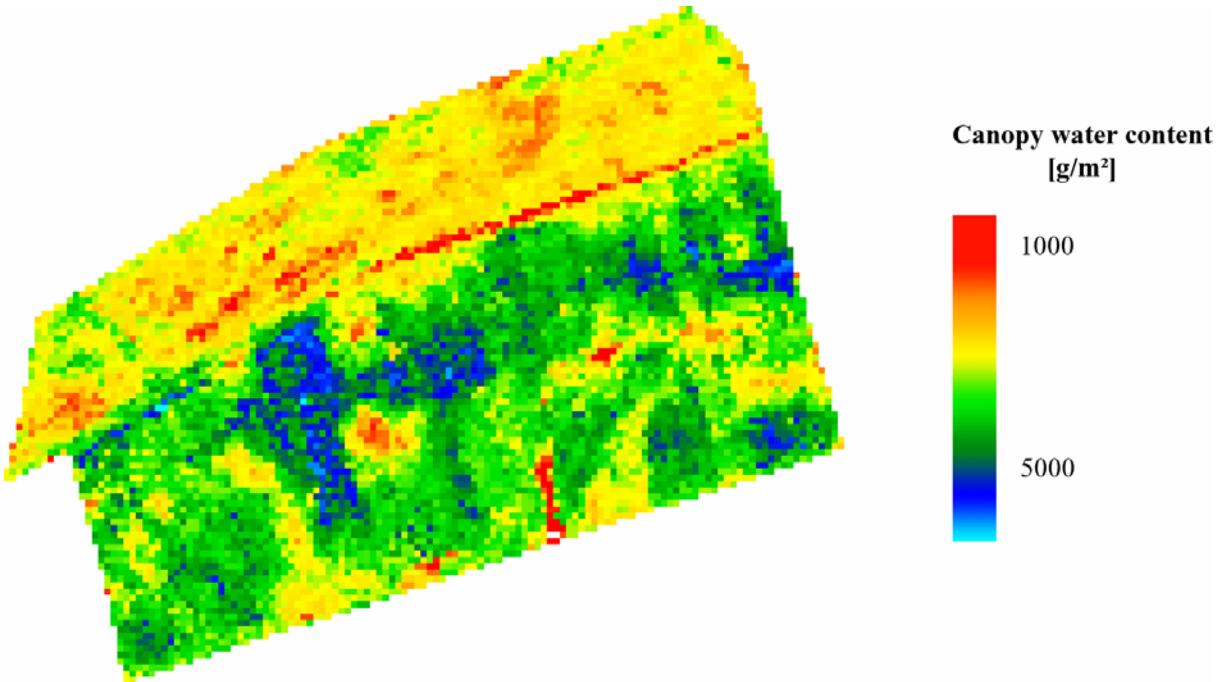

Figure 7: Estimated water content of wheat canopies

CONCLUSIONS

It was demonstrated that the WI introduced by Peñuelas et al. can be applied to predict the water content [g/m²] of wheat canopies with high acccuracy. Additionally, it allows a fast and non-destructive analysis. Both are also true for a modified index version using the variable wavelength of maximum absorption in the 970 nm-water absorption feature.

R^2 of the cross-validated estimations of water content - derived from spectrometer data - was 0.896 for the WI and 0.869 for the modified index. For its simplicity and precision, the tested approach seems to be operational for a low cost- and field-wise estimation, even much more appropriate than traditional time-consuming field methods.

Realistic water contents were estimated on the base of HyMAP image data; the spatial pattern of water content was explainable by the morphology of the investigated field. Thus, no scaling problem is evident when transferring the approach to HyMAP data.

ACKNOWLEDGEMENTS

We would like to acknowledge the funding provided by the German Research Foundation (SFB 522: Umwelt und Region) and the Forschungsfonds of the University of Trier. Many thanks to the “Maschinenring” of the Trier region for its help selecting suitable fields. The farmers involved in this study we would like to thank for their corporation. Special thanks to Jan Krause, Andreas Marx and Sebastian Mader for field work and pre-processing the HyMAP data.

References

i Peñuelas J, J Pinol, R Ogaya & I Filella 1997. Estimation of plant water concentration by the reflectance Water Index WI (R900/R970). International Journal of Remote Sensing, 18:2869-2875

ii Willert D J von, R Matyssek & W Herppich, 1995. Experimentelle Pflanzenökologie. Stuttgart, New York

iii Idso S B, R D Jackson & R J Reginato, 1977. Remote sensing of crop yields. Science, 196:19-25

iv Jacquemoud S, F Baret, B Andrieu, F M Danson & K Jaggard, 1995. Extraction of Vegetation Biophysical Parameters by Inversion of the PROSPECT + SAIL Models on Sugar Beet Canopy Reflectance Data. Application to TM and AVIRIS Sensors. Remote Sensing of Environment, 52:163-172

v Zarco-Tejada P J & S L Ustin, 2003. Modelling canopy water content for carbon estimates from MODIS data at land EOS validation sites. In. International Geoscience and Remote Sensing Symposium, IGARSS `01, 342-344

vi Peñuelas J, I Filella, C Biel, L Serrano & R Savé, 1993. The reflectance at the 950-970nm region as an indicator of plant water status. International Journal of Remote Sensing, 14:1887-1905

vii Gao B-C, 1996. NDWI – A normalized difference water index for remote sensing of vegetation liquid water from space. Remote Sensing of Environment, 58:257-266

viii Curran P, 1994. Imaging Spectrometry. Progress in Physical Geography, 18(2):247-266

ix Tian Q, Q Tong, R Pu, X Guo & C Zhao, 2001. Spectroscopic determination of wheat water status using 1650-1850nm spectral absorption features. International Journal of Remote Sensing, 22:2329-2338

x Pu R, S Ge, N M Kelly & P Gong, 2003. Spectral absorption features as indicators of water status in coast live oak (Quercus agrifolia) leaves. International Journal of Remote Sensing, 24:1799-1810

xi Goa B-C & F H Goetz, 1990. Column atmospheric water vapour and vegetation liquid water retrieval from airborne imaging spectrometer data. Journal of Geophysical Research, 95:155-162

xii Savitzky A & M J Golay, 1964. Smoothing and differentiation of data by simplified least square procedure. Analytical Chemistry, 36:1627-1638

xiii Gamon J A, R O Green, D A Roberts & L Serrano, 1995. Deriving photosynthetic function from calibrated imaging spectrometry. In: Proceedings of the International Colloquium, Photosynthesis and Remote Sensing, 28-30 August 1995, Montpellier (France), 55-60 xiv Sonnenschein R, 2004. Bestimmung des Wassergehaltes von Weizenbeständen aus Spektrometermessungen (unpublished Diploma thesis, University of Trier). 73 pp.

xv Strachan I B, E Pattey & J B Boisvert, 2002. Impact of nitrogen and environmental conditions on corn as detected by hyperspectral reflectance. Remote Sensing of Environment, 80:213-224

xvi Deutscher Wetterdienst, 2003. Deutsches Meteorologisches Jahrbuch 2000. Offenbach am Main

xvii Cocks T, R Jenssen, A Stewart, I Wilson & T Shields, 1998. The HyMAP™ airborne hyper-spectral sensor: the system, calibration and performance. In: Proceedings of the 1st EARSEL Workshop on Imaging Spectroscopy, Zurich, October 1998, 37-42

xviii Schläpfer D & R Richter, 2002. Geoatmospheric Processing of Airborne Imaging Spectrometer Data Part 1: Parametric Orthorectification. International. Journal of Remote Sensing, 23:2609-2630.

xix Mattew M W, S M Adler-Golden, A Berk, S C Richtsmeier, R Y Levine, L S Bernstein, P K Acharya, G P Anderson, G W Felde, M P Hoke, A Ratkowski, H-H Burke, R D Kaiser & D P Miller, 2000. Status of Atmospheric Correction Using a MODTRAN4-based Algorithm. Proc. SPIE, 4049:199-207.